 DOI: 10.1002/masy.200650512

Atomistic Simulation of Bulk Mechanics and Local Dynamics of Amorphous Polymers

Alexey V. Lyulin,[*1] *J. Li,*[1,2] *Tim Mulder,*[1] *Bart Vorselaars,*[1] *M.A.J. Michels*[1]

Summary: In order to have better insight into the polymer specifics of the dynamic glass transition molecular dynamics (MD) computer simulations of three glass-formers have been carried out: low-molecular-weight isopropylbenzene (iPB), brittle atactic polystyrene (PS) and tough bisphenol A polycarbonate (PC). Simulation of the uniaxial deformation of these mechanically different types of amorphous polymers shows that the mechanical experimental data could be realistically reproduced. Now the objective is to study the local orientational mobility in the non-deformed isotropic state and to find the possible connection of the segmental dynamics with the different bulk mechanical properties. Local orientational mobility has been studied via Legendre polynomials of the second order and CONTIN analysis. Insight into local orientational dynamics on a range of length- and time scales is acquired. The fast transient ballistic process describing the very initial part of the relaxation has been observed for all temperatures. For all three simulated materials the slowing down of cage escape (α-relaxation) follows mode-coupling theory above T_g, with non-universal, material-specific exponents. Below T_g universal activated segmental motion has been found. At high temperature the α process is merged with the β process. The β process which corresponds to the motions within cage continues below T_g and can be described by an activation law.

Keywords: computer modeling; glass transition; mechanical properties; relaxation

Introduction

The glassy state of matter and the glass transition itself are still great, ill-understood problems in condensed-matter physics. The transformation from a liquid to a glass takes place in a continuous manner. Its characteristic feature is the fact that the structural relaxation times and the viscosity of the liquid increase progressively as the temperature is lowered[1–4], and in a fixed time window seem to diverge at finite temperature. At present, there is no unified theoretical understanding of the molecular mechanisms that give rise to the tremendous increase of relaxation times in simple glass-formers. In thermodynamic approaches to the glass transition[5] configurational entropy is associated with the possibility for a system to explore different disordered states. There are vibrational motions around each minimum with occasional hops between two minima. In this picture, the configurational entropy is simply related to the number of minima by the usual Boltzmann formula. The essential idea of the mode-coupling theory (MCT) of glass transition[6] is that the transition towards a glass is a purely dynamical one. The ideal MCT attributes the slowing down of particle motion at low temperatures to ''backflow'' collective-particle motion which eventually causes a structural arrest of the dynamics.

[1] Group Polymer Physics, Eindhoven Polymer Laboratories and Dutch Polymer Institute, Technische Universiteit Eindhoven, P.O. Box 513 5600 MB Eindhoven, The Netherlands

[2] Department of Macromolecular Science and Key Lab of Molecular Engineering of Polymers, Ministry of Education of China, Fudan University, Shanghai 200433, China

For polymers, with their complex microstructure, the glass transition is, of course, even less understood It is, however, one of the most important properties of amorphous polymers both practically and theoretically, because it involves a dramatic slowing down in the motion of chain segments (the dominant relaxation time τ becomes larger than about 10^2 s), whereas one can hardly see any accompanying change in the static structure[7].

Understanding the mechanisms at work on local segmental scale is one of the most important challenges, both for the low-molecular-weight and for polymeric glasses. The extended mode-coupling theory[6] seems to be applicable to polymers, explaining temperature scaling of different relaxational processes; however, its applicability is limited to a quite narrow temperature range. Theoretical and simulation results[6,7] provide direct evidence that the collective character of molecular motion is responsible for the slowing down of mobility in model polymer glasses but conclusions are still made mainly on toy-polymer models; although the cooperative dynamic behaviour in the vicinity of the polymer glass transition is a generic physical phenomenon, polymer-specific chemistry plays an important role in practice.

Understanding the connection between polymer chemical structure, local segmental mobility and bulk mechanical properties will open up new ways of designing materials with extreme ultimate properties. For example, from mechanical experiments it is concluded that polystyrene (PS) is brittle and that polycarbonate (PC) is ductile, but the underlying mechanisms of this difference between the two polymers remain unclear[8–10]. Our recent studies[11–13] on molecular dynamics (MD) simulation of an atomistic model of a polystyrene melt help to understand the details of segmental mobility in the glassy state.

The simulations show that above T_g the times of the main relaxational processes for this polymer all follow the same universal power law as the characteristic translational diffusion time and the characteristic time of dynamic scattering, in good agreement with the predictions of MCT. The character of mobility is qualitatively changed below T_g: when crossing T_g the divergence of the relaxation times – as predicted by MCT- is not observed, but all relaxational segmental dynamics starts to follow one and the same activation law.

In order to investigate the possible polymer-connectivity-related effects in the glassy dynamics we have performed an MD simulation of the low-molecular weight analogue of PS, isopropylbenzene (iPB), at an isotropic atmospheric pressure and in a wide temperature range. The choice of iPB was motivated by the fact that its typical time scale of the orientational relaxation is within the simulated time window, which allows us to separate different relaxational processes with sufficient precision. We also performed MD simulations for the two mentioned mechanically very different glassy polymers – the typical brittle, atactic polystyrene, and the typical ductile, bisphenol A polycarbonate, both in the non-deformed state and under the uniaxial deformation. Our interest is in the study of the experimentally observed different strain-softening and strain-hardening behaviour of PS and PC, and possible links of this different bulk mechanics with differences in mobility on the segmental level.

Algorithm and Simulation Details

United-atom models are used in the present study; for iPB and PS the model and the force field are described in detail by Lyulin et al.[11], for PC the force field of Hutnik et al.[14] is used. The simulation details are mentioned in[11–13]. In short, a low-molecular weight analogue of polystyrene, isopropylbenzene (iPB), C_9H_{12}, has been simulated for $N = 80$ and $N = 640$ molecules (720 and 5760 united atoms, correspondingly), in a wide range of temperatures both above and below T_g. The MD simulation has been performed for a model PS melt consisting of 1–8 polymer chains of $N_p = 80$–160 monomers each (molecular weight $\sim$ 8300–16600 Da, about one entanglement length) and its periodic images. The stereochemic configurations of the aro-

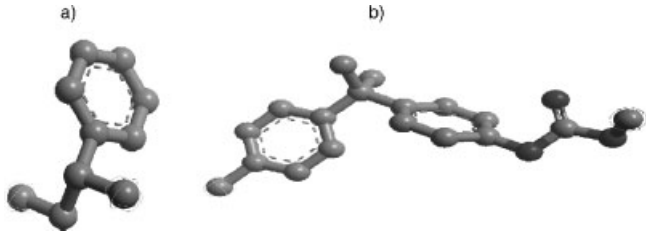

Figure 1.
Monomer units for the united-atom models of PS (a) and PC (b) used in the present study. The iPB melt was also simulated using the united-atom polystyrene force field.

matic groups were generated at random so that the ratio of the number of *meso* to *racemic* dyads was near unity. 64 chains of $N_p = 10$ monomers (about one entanglement length, 64×10 system) and 8 chains of $N_p = 80$ monomers (about 8 entanglement lengths, 8×80 system) have been used for the PC melt. The leap-frog velocity Verlet algorithm[15] has been used to integrate the Newtonian equations of motion with the time step of $\Delta t = 4$ fs. The Berendsen *NPT* MD algorithm[15] has been used, with time constants $\tau_T = 0.5$ ps and $\tau_P = 1$ ps. Some runs have been performed using the collisional thermostat[13].

The iPB melt was prepared by melting of the initial lattice configuration at $T = 370$ K (well above the corresponding T_g) and atmospheric pressure for about 15 ns. The equilibration of the polymer samples above T_g is very important. For the present calculations well-equilibrated initial structures have been taken from our previous studies[11]. In order to check the quality of equilibration, some runs have been performed using initial structures generated by the MSI Materials Studio™ Amorphous Cell interface. The calculated final conformational properties and final densities were identical to those produced in the present study. PC samples were prepared by isotropic compression of initially extended chains arranged in a lattice. In order to further check the equilibration of the initial polymer-melt structures we have started to use the new effective end-bridging Monte Carlo algorithms[16]; this study is in progress now.

Step-wise cooling was used to produce the iPB glasses from the initial liquid state at $T = 370$ K, with steps of 30 K down in temperature, followed by an equilibration of about 4 ns. Both the PS and PC polymer melts have been cooled down with a continuous cooling rate of 5×10^{-2} K/ps from the initial high-temperature liquid state at $T = 630$ K. Also step-wise cooling, with steps down in temperature of about 10 K, followed by an equilibration of about 20 ns, has been performed, but only for a PS melt.

Uniaxial deformation with constant deformation velocity $\dot{L} = 0.005$ Å/ps was applied along one (X, Y or Z) of the axes to five independent sets of relaxed isotropic PS and PC samples, at $T = 300$ K, well below the corresponding simulated glass transition temperatures; here $L(t) = L_0 + \dot{L}t$ is the instant length of the simulation box parallel to the direction of the applied tension and L_0 denotes the initial value of the box length prior to the application of tension. For the resulting fifteen different deformed samples the nominal strain parallel to the direction of deformation has been measured as

$$\gamma_L = \frac{L - L_0}{L_0} \times 100\%.$$

Results and Discussion

Uniaxial Deformation

The uniaxial deformation was applied to the relaxed polymer samples at room

temperature ($T = 300$ K). After the application of the deformation, the initial elastic regime for both polymers is clearly seen for extensions up to ~3%, and is followed by the onset of plastic flow in the yield point, Figure 2. At $T = 300$ K the simulated Young modulus is ~2.9 GPa for PS and ~2.2 GPa for PC, which is comparable to the experimental values at room temperature of 3.2–3.4 GPa and 2.34 GPa for PS and PC, respectively[17]. In spite of the enormous difference in deformation rate[18], the simulated values of the yield stresses (~100 MPa for PS and ~70 MPa for PC) are also comparable to the experimental ones at the same temperature (yield stress of 95~MPa for PS and 65~MPa for PC).

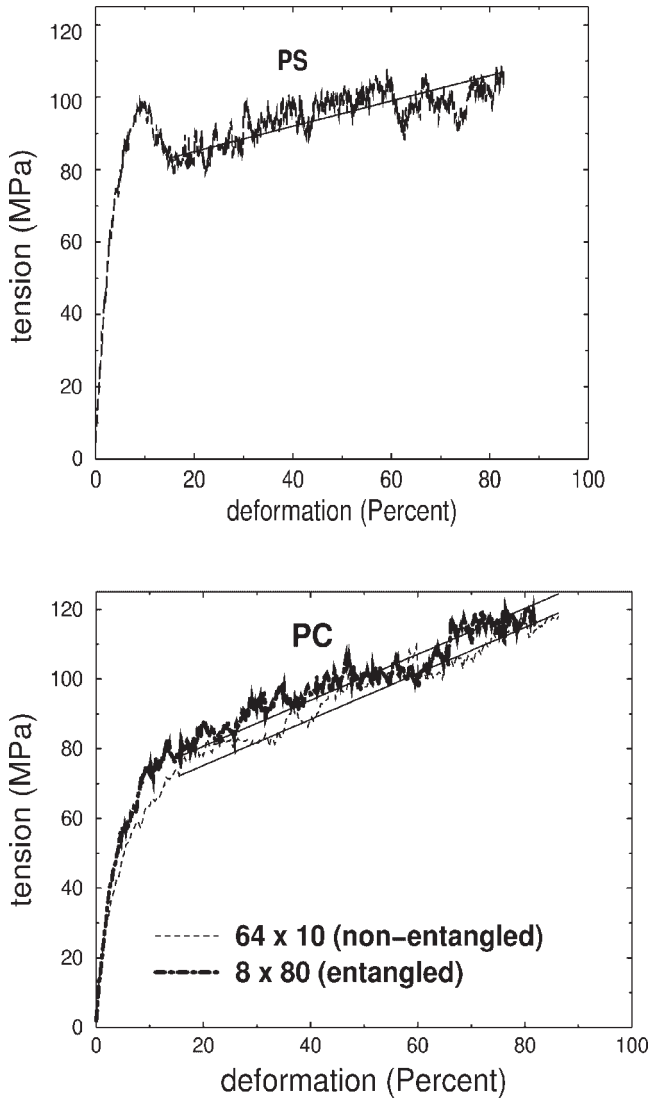

Figure 2.
Stress-strain behaviour of a non-entangled PS melt (4 chains × 160 monomers each) (top) and two specimens of PC of different molecular weight (bottom) at $T = 300$ K. Strain softening is clearly seen for the PS sample, and is clearly absent for PC. The straight lines are least-square fits of the data in the strain-hardening regime.

After the yield point pronounced strain softening is clearly seen in Figure 2 for simulated PS, with a stress drop of about 20 MPa. Such a softening is not present for PC. For both polymers strain hardening is clearly seen at larger extensions (above $\gamma_L \sim 15\%$). The strain-hardening modulus G_R is usually defined[19] as the slope of the curve at large strains (deformation above 15% in the present simulations) of the true stress σ versus $\lambda^2 - \lambda^{-1}$, $\sigma = G_R(\lambda^2 - \lambda^{-1})$, where $\lambda = \frac{L}{L_0}$. The present simulation data at $T = 300$ K give the value $G_R = 12.0 \pm 0.5$ MPa for PS, almost twice lower than the simulated value for PC.

These results may be compared with available experimental uniaxial-compression data of van Melick et al.[19], which give $G_R = 13$ MPa for PS and $G_R = 29$ MPa for PC at room temperature.

Due to the uniaxial extension the translational mobility of the monomers is different from that in the undeformed case (the trivial contribution to the parallel mean square translational displacements (MSTD), due to the convective motion of the monomers in the direction of the deformation, was eliminated). For both polymers the deformation does not influence significantly the translational mobility below the yield point, Figure 3. Changes occur only in the post-yield response: for the parallel MSTD the onset of the cage escape starts significantly earlier as compared to the isotropic case. For the PS glass the uniaxial mechanical deformation leads to an acceleration of the parallel diffusion by more than one order of magnitude. For the PC glass the deformation also influences the mobility, but the acceleration of the parallel diffusion is much weaker as compared to PS.

We see (Figure 3) that the mechanical deformation leads to differences in the local translational segmental mobility for the two polymers. In the reminder of the paper we focus on the segmental orientational relaxation in the low-molecular weight iPB and both polymers in the nondeformed state. As compared to the polymer samples, iPB has a rather high mobility even in the vicinity of the glass transition; the characteristic relaxation times of iPB are well within the MD-simulated time window. The orientational relaxation of iPB may be accurately simulated, which allows us to make meaningful conclusions about the character of the local dynamics (and its polymer specifics) when approaching T_g.

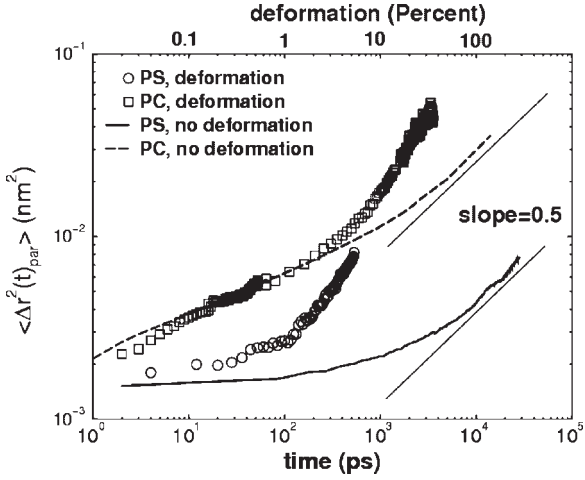

Figure 3.
The stochastic contributions to the MSTD in the direction of the deformation, averaged over all backbone monomers for PS and PC, 8 × 80 samples, $T = 300$ K. Lines represent the corresponding MSTD along one of the Cartesian coordinates in the isotropic case.

Glass Transition

The MD simulations were used to study the glass transition in all systems. The temperature dependence of the specific volume for iPB, PS and PC cooled down with different cooling rates (see above), is monitored in Figure 4. The glass-transition temperature was measured as an intersection of the linear fits to the low-temperature and high-temperature simulation data. For low-molecular-weight iPB the simulated T_g (175 K) is significantly lower as compared to that of PS (375 K) (we stress that our goal here was not to reproduce the experimental value of T_g for any compound, but rather see the difference between a polymer and its low-molecular-weight analogue simulated with the same force field). The values of T_g produced by the step-wise cooling are lower as compared to the continuous-coolingT_g, because the effective cooling rate of the step-wise cooling is smaller. The

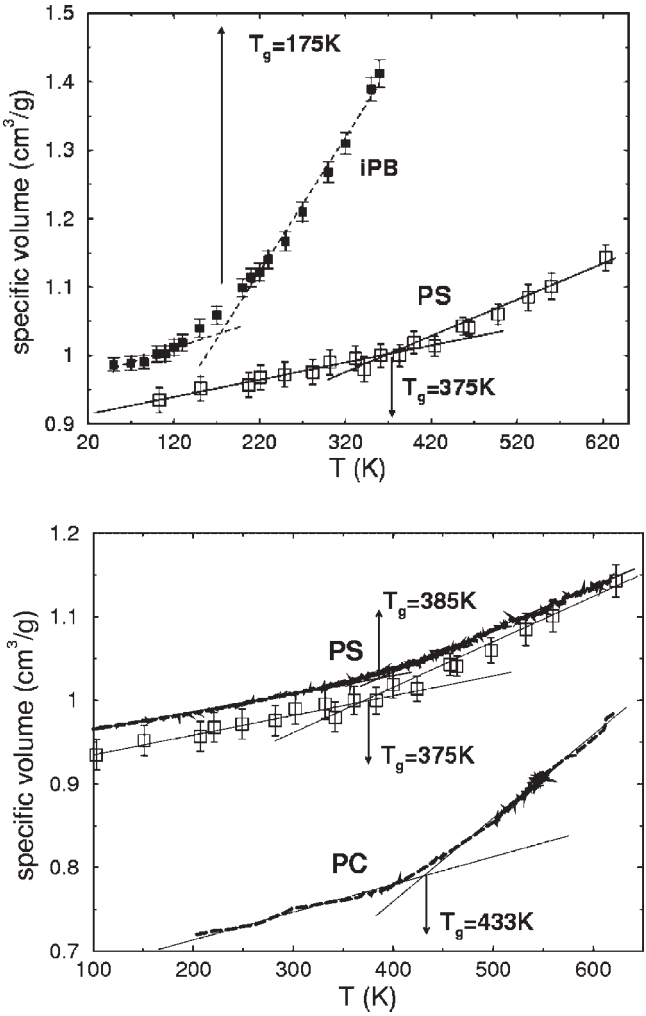

Figure 4.
Temperature dependence of the specific volume for iPB and PS melts (top) produced with step-wise cooling. Continuous cooling with a cooling rate of 5×10^{-2} K/ps was also used for PS and PC melts (bottom figure, solid curves). The simulated values of T_g are indicated by arrows. Straight lines reproduce linear fits to the data.

detailed discussion of the observed cooling-rate dependence can be found elsewhere[13,20].

Local Orientational Mobility

The local orientational mobility of the iPB in the vicinity of its glass transition has been studied in detail. For this purpose we analyzed the orientational relaxation of iPB with the help of Legendre polynomials of the second order (autocorrelation functions, ACFs)

$$P_2(t) = \left\langle 3/2(\mathbf{b}(0)\mathbf{b}(t))^2 - 1/2 \right\rangle, \quad (1)$$

where **b** is the unit vector directed along the main-chain bond or along the phenyl side group (in iPB or PS, see further sections) and brackets denote a position and time averaging. Kohlrausch-Williams-Watts (KWW)[21] stretched-exponential functions have been used to fit the final parts of the ACFs at different temperatures,

$$P_2(t) = \exp(-(t/\tau_2)^{\beta}), \quad (2)$$

where τ_2 is the characteristic orientational relaxation time and β is the parameter effectively taking into account the non-exponential nature of the relaxation process (the temperature dependence of this β parameter is a subject of a separate study).

Each ACF is also analyzed using the CONTIN[22] technique

$$P_2(t) = \int_{-\infty}^{+\infty} F(\ln\tau)\exp(-t/\tau)d(\ln\tau) \quad (3)$$

where $F(\ln\tau)$ is a normalized distribution function of relaxation times. This function is shown for iPB in Figure 5. Three relaxational processes can be identified at each temperature. The very fast transient process (times less than 1 ps) is connected to the ballistic motion of beads, and is purely determined by the thermal velocity of the united atoms at each prescribed temperature. This transient process has a very weak temperature dependence (Figure 5, right, circles). On the other side of the spectrum of relaxation times is the so-called α process. The temperature dependence of the relaxation times of the α process above T_g is clearly non-Arrhenius, and can be fitted by the Vogel-Fulcher-Tamman (VFT) empirical equation, Figure 5

$$\tau^{-1} \sim \exp(-E_a/k_B(T - T_0)) \quad (4)$$

with $E_a = 1$ kJ/mol and $T_0 = 150\ \mathrm{K} < T_g = 175$ K.

The idealized mode-coupling theory[6–7] predicts an algebraic divergence of the characteristic relaxation times at some critical temperature T_c above the actual T_g,

$$\tau \sim (T - T_c)^{-\gamma}. \quad (5)$$

From a two-parameter fit to the simulated α-relaxation data the values of T_c and γ are extracted, giving $T_c \sim 181$ K (above the simulated value of T_g) and the critical exponent $\gamma \sim 1$. The value of the critical exponent is significantly lower as compared to those for PS and PC, as will be shown below. The MCT-like fit (5) is very close to the VFT fit produced by Equation 4, and is not shown in Figure 5 for clarity. Below T_g the MCT does not work, as it predicts a divergence of the relaxation times. Such a divergence is absent in the present simulations. Instead, one can see that the character of the α process is qualitatively changed from the MCT-like collective process above T_g to an activated one below T_g. The simple activation law is used to fit the simulation data for the α process with $E_a = 2.7$ kJ/mol, Figure 5.

The temperature dependence of the characteristic times of the third (β) process is also extracted from the CONTIN analysis. This dependence can be described by a simple activation law, both below and above T_g, with $E_a = 6.8$ kJ/mol. From Figure 5 it is seen that at high temperature the α and β processes are merged, and start to split at temperatures slightly above T_g.

How does this picture change for specific polymers? The analysis explained above for iPB has been implemented here also for PS and PC. As in the case of iPB, three relaxational processes can also be identified there at each of the simulated temperatures: the very fast transient process, the β process, and, finally, the α process, Figure 6. Not surprisingly the absolute values of the

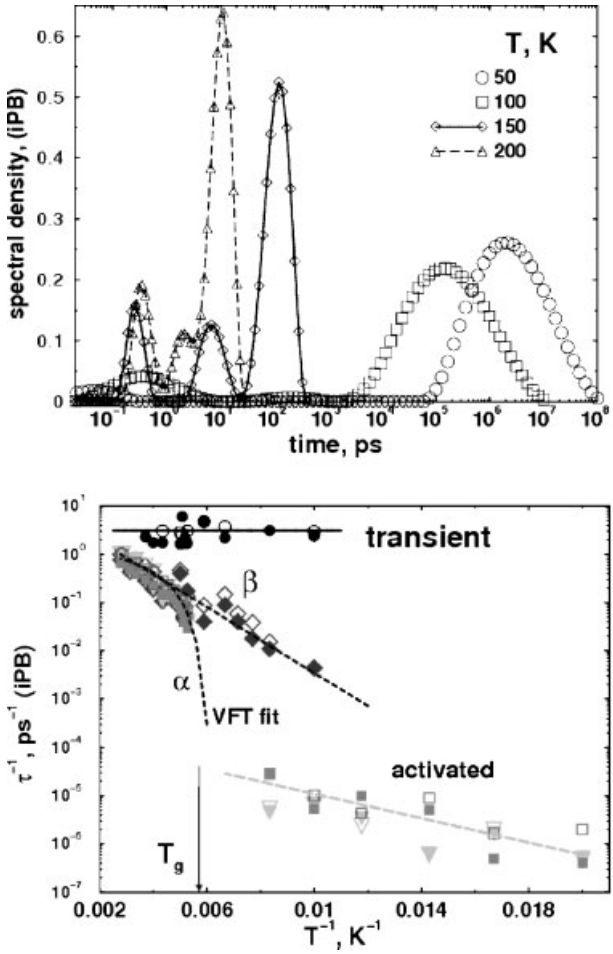

Figure 5.
Normalized distribution function of the relaxation times for the $P_2(t)$ ACF for the backbone bond of iPB at different temperatures (top). Three relaxation processes are clearly seen at all temperatures. The temperature dependence of the characteristic relaxation times is also shown (bottom), for the backbone (closed symbols) and the side-group (open symbols) vectors: times for the β and transient processes are calculated from the position of the corresponding maxima in the CONTIN distribution functions; times for the α and activated processes are calculated from CONTIN (inverse triangles) and from KWW fits (squares). The VFT fit for the α process above T_g is also shown. Straight dashed lines represent an activation-law fit for the β- and activated relaxation processes.

ballistic time (transient relaxation process) for polymers are very close to those for the low-molecular-weight compound. As in the case of iPB, their temperature dependences are also very weak (Figure 6). The temperature dependence of the β process is very close to the activation law for both polymers, but the values of the activation energies are much larger as compared to iPB ($E_a = 20$ kJ/mol for PS and $E_a = 28$ kJ/mol for PC as compared to $E_a = 6.8$ kJ/mol for iPB).

At high temperature the β process is merged with the α process for both polymers, the processes start to split at temperatures well above T_g. MCT fits for α process hold for both polymers above $T_c > T_g$. (see Figure 6), with the values of the critical exponents much larger as compared to iPB ($\gamma \sim 2$ for PC, $\gamma \sim 3$ for

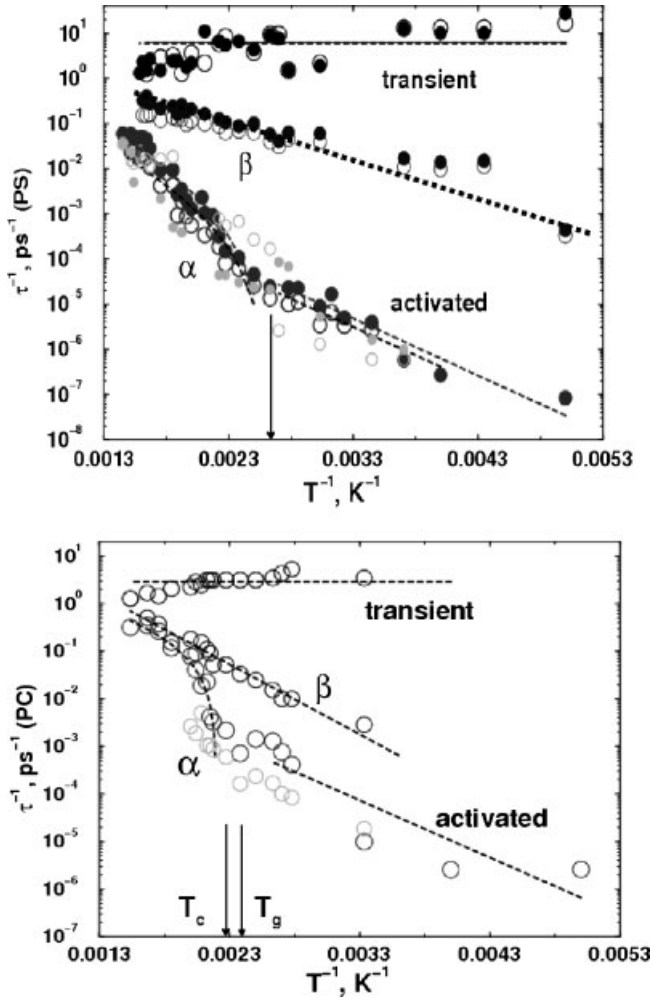

Figure 6.

Temperature dependence of three relaxation processes for the backbone (closed symbols) and the side-group vectors (open symbols) of PS (top, 1×80 melt) and PC (bottom, 64×10 melt). Times for the β and transient processes are calculated from the position of the corresponding maxima in the CONTIN distribution functions; times for α and activated processes are calculated from CONTIN (grey open and closed circles) and from the KWW fit (black open and closed circles). The MCT fit for the α process above T_g (dashed line) is shown for both polymers. Straight dashed lines represent the activation-law fit for the β- and activated relaxation processes.

PS and $\gamma \sim 1$ for iPB). The VFT fits, Equation 4, also hold (they are not shown in Figure 6 for clarity), but with the values of T_0 much lower than the corresponding values of T_g for both polymers. As in the case of iPB the α process in polymers is continued below T_g, but the character of this relaxation is changed from the MCT-like collective motion to the activated, hopping-like behaviour. Again, qualitatively this picture is similar to that for the low-molecular-weight glass, but the activation energy is one order of magnitude larger: $E_a = 24$ kJ/mol for PS, $E_a = 23$ kJ/mol for PC as compared to $E_a = 2.7$ kJ/mol for iPB.

Conclusions

Detailed atomistic molecular dynamics simulations have been performed for chem-

ically realistic models of two typical amorphous polymers, atactic polystyrene and bisphenol A polycarbonate, and for the low-molecular-weight analogue of polystyrene, isopropylbenzene. We have studied the different bulk mechanics of the two polymers in the glassy state together with their mobilities on the segmental level. In spite of the difference between computational and experimental deformation rates the widely different bulk mechanical behaviour could be realistically simulated. For PS the initial softening after the yield point is concomitant with a significant increase of the local segmental mobility in the direction of deformation. This effect is less for PC.

The main focus of this paper is on the computational study of the orientational mobility of these glasses in the isotropic, non-deformed state. CONTIN analysis of the distribution functions of the characteristic orientational relaxation times reveals the existence of three different relaxation processes for all three compounds: an initial ballistic process at very short times, followed by the β relaxation (motions within the cage) and, finally, the relaxation of the cage itself (the α process). The temperature dependence of the characteristic times of the ballistic process is very weak. The β relaxation is an activated process which continues below T_g, and which merges with the α process at high temperature. This merging is observed for all three compounds. The predictions of MCT are also validated for each of the three systems, but with different, structure-specific values of the critical exponents. The value of the critical exponent is $\gamma \sim 1$ for iPB and increases significantly for polymers ($\gamma \sim 2$ for PC and $\gamma \sim 3$ for PS). Similarly, the crossover from collective α process above T_g to the activated type of segmental relaxation below T_g is found for the polymers, as well as for the low-molecular weight melt, but with activation energies very different for the polymer- and low-molecular-weight glasses, respectively.

The direct connection of the (different) segmental mobilities to the macroscopically different and rate-dependent mechanical behaviour will still require many years of research. Nevertheless, in our simulations two regimes of stress-strain behaviour can be distinguished for both polymers if the entanglements are disregarded: the initial viscoelastic regime of (very small) homogeneous deformation and the second, plastic (post-yield) regime. The latter regime can in the present results clearly be identified with a forced and accelerated motion of the chain segments out of their cages. The transition between two regimes is probably more gradual for PC as compared to PS because of the larger intra-chain flexibility and smaller chain cross-section. In this second regime PC has more hardening probably a.o. because of the larger population of extended trans-zigzag conformers[23] and/or larger distance from the corresponding glass-transition temperature[19]. The pronounced softening for PS could probably be connected to the onset just after the yield point of orientation of the phenyl rings in the direction perpendicular to the applied deformation. In other words, while showing common physical mechanisms our results give further evidence of the importance of the details of the inter- and intrachain interactions (torsions, Coulomb forces and excluded volume) for the different post-yield behaviour of chemically-specific polymers. The detailed analysis of this is a subject of our future study.

This work forms part of the research programme of the Dutch Polymer Institute (project 487). We acknowledge the SARA High Performance Computing Centre in Amsterdam for providing the generous amount of the necessary CPU time.

[1] M.D. Ediger, C.A. Angell, S.R. Nagel, *J. Phys. Chem* **1996**, *100*, 13200.
[2] C.A. Angell, *Science* **1995**, *267*, 1924.
[3] F.H. Stillinger, *Science* **1995**, *267*, 1935.
[4] B. Frick, D. Richter, *Science* **1995**, *267*, 1939.
[5] J.-L. Barrat and J.-P. Hansen, "*Basic Concepts for Simple and Complex Liquids*", Cambridge University Press, 2003.
[6] W. Götze, *J. Phys.: Condens. Matter.* **1999**, *11*, A1.

[7] K. Binder et al., *Philosophical Magazine* **1998**, *B77*, 591.
[8] H.H. Kausch, *Polymer Fracture*, Springer-Verlag, Heidelberg, 1987.
[9] ''*Reinforcement of Elastomers*'', G. Kraus Ed., Interscience, 1965.
[10] R.J.M. Smit, ''*Toughness of Heterogenic Polymeric Systems: a Modelling Approach*'', Ph.D. thesis, Eindhoven University of Technology, Eindhoven, the Netherlands, 1998.
[11] A.V. Lyulin, M.A.J. Michels, *Macromolecules* **2002**, *35*, 1463.
[12] A.V. Lyulin, N.K. Balabaev, M.A.J. Michels, *Macromolecules* **2002**, *35*, 9595.
[13] A.V. Lyulin, N.K. Balabaev, M.A.J. Michels, *Macromolecules* **2003**, *36*, 8574.
[14] M. Hutnik, A. S. Argon, U. W. Suter, *Macromolecules* **1991**, *24*, 5956.
[15] M. P. Allen, D. J. Tildesley, ''*Computer Simulation of Liquids*'', Clarendon Press, Oxford, 1987.
[16] M. Doxastakis, V.G. Mavrantzas, D.N. Theodorou, *J. Chem. Phys.* **2001**, *115*, 11352.
[17] I.M. Ward, D.W. Hadley, *An Introduction to the Mechanical Properties of Solid Polymers*, J. Wiley and Sons, England, 1993.
[18] J. Rottler, M. O. Robbins, *Phys. Rev. E* **2003**, *68*, 011507.
[19] H. G. H. van Melick, L. E. GovaertH. E. H. Meijer, *Polymer* **2003**, *44*, 2493.
[20] A.V. Lyulin, B. Vorselaars, M.A. Mazo, N.K. Balabaev, M.A.J. Michels, *Europhys. Lett.*, **2005**, *71*, 618.
[21] G. Williams, D.C. Watts, *Trans. Faraday Soc.* **1970**, *66*, 80.
[22] S. Provencher, *Comput. Phys. Commun.* **1982**, *27*, 213.
[23] J.I. McKehnie, R.N. Haward, D. Brown, J.H.R. Clarke, *Macromolecules* **1993**, *26*, 198.

